IEEE Access
Multidisciplinary | Rapid Review | Open Access Journal

Received December 10, 2016, accepted January 3, 2017, date of publication January 20, 2017, date of current version July 7, 2017.

Digital Object Identifier 10.1109/ACCESS.2017.2655040

Novel Anti-Deception Jamming Method by Measuring Phase Noise of Oscillators in LFMCW Tracking Radar Sensor Networks

MAHDI NOURI, (Student Member, IEEE), MOHSEN MIVEHCHY, (Member, IEEE), AND MOHAMAD F. SABAHI, (Member, IEEE)
Department of Electrical Engineering, University of Isfahan, Isfahan, Iran
Corresponding author: Mohsen Mivehchy (mivehchy@eng.ui.ac.ir)

ABSTRACT In this paper, the effects of phase noise difference in receiving signals are introduced to discriminate targets. Oscillators and signal sources have their own phase noise levels and specific patterns. This property can be used for discriminating a real target from the airborne digital radio frequency memory (DRFM) in continuous wave tracking radar sensor networks with linear frequency modulation. A simulated signal made through complex circuits by DRFM has higher phase noise with different patterns. To investigate the phase noise level of oscillators, a system is provided to measure the phase noise. Then, the probability of detection (P_D) and the probability of false alarm (P_{fa}) can be achieved by defining an appropriate threshold to evaluate the performance of discriminating between real targets and DRFM targets. The phase noise powers are measured through the same sets of circuits and coherent time periods in various radar sensor systems. To control the amplitude fluctuation of the received signal, the normalization of signal phase power is defined in phase noise bandwidths. The likelihood ratio test is used for target discrimination by a threshold level to achieve the minimum P_{fa} of target discrimination. The proposed method has a simple structure without any additional complexities, and is easily compatible with common radar systems. Two real DRFM systems are used to evaluate the performance of the proposed method in both the L-band and X-band frequencies. The presented results are investigated in different ranges, Doppler frequencies, signal-to-noise ratios, and signal-to-jammer ratios. The experimental results prove the capability of proposed method in radar sensor networks.

INDEX TERMS Digital radio frequency memory, phase noise measurement, false target, radar oscillator, linear frequency modulation.

I. INTRODUCTION

In modern radar systems, accurate target detection is very important to differentiate among strong noise, clutter, and, in particular, jamming signals from the environment [1]. Radars can be categorized into two types: pulse radar and continuous wave (CW) radar. Generally, the simple kinds of CW radars have poor range detection. On the other hand, use of linear frequency modulation (LFM) in wideband radar systems or phase code for better range detection offers many advantages. Tracking radar performance declines with active and passive electronic counter measure (ECM) methods by producing jamming signals. ECM methods are improving at a rapid pace due to improvements in military equipment [2], [3]. Electronic counter-counter measures (ECCM) methods, on the other hand, are used to work against ECM attacks [2]. One of the effective uses of active ECM methods is deception jamming. The most applicable and flexible method senses transmitted radar signal and simulates false target echoes using the digital radio frequency memory (DRFM) technique. This ''tricks'' the tracking radar to ignore the real target besides allows the jamming signals to saturate the radar processors [4]. DRFM is also denoted as the repeat-back jammer [5], [6]. A group of ranges and Doppler frequencies are used in DRFM to produce a bunch of replicas of received signals to deceive the radar system to concentrate on a fake target instead. Thus, tracking moving target indicator (MTI) and CW radars are threatened by DRFM jammers [7], [8].

Frequency hopping (FH) is a precedent technique with acceptable performance in a jamming environment [9], [10]. Parameters like modulation method, FH bandwidth,

and hopping rate have an influence in the performance of this method. These various parameters cause some weaknesses such as pulse repetition interval (PRI) variation and peak-to-average power ratio (PAPR). Furthermore, higher spectrum consumption increases the bandwidth for hopping. Arbitrarily varying the hopping pattern by an arbitrary form resists jamming. Binary random phase-coded modulation is one of the applicable ECCM methods to thwart DRFM signals [10]–[12].

Use of phase-code diversity in the pulse has good performance for target discrimination without Doppler processing. Another technique consists of random pulse repetition interval (PRI) waveforms, which decreases the jamming efficiency [13]. However changing the PRIs causes range ambiguity by average power reduction for a long time. Pulse diversity is an effective technique used to counter DRFM [14]–[16]. Orthogonal sub-pulses in consecutive PRIs are used in this method. Hence, transmitted signal patterns cannot be easily achieve by DRFM jammers. However, it is not useful when Doppler processing is required, because MTI filter needs several PRIs to give accurate Doppler frequency. Changing pulses in every PRI causes higher range sidelobe, which decreases the signal-to-jammer ratio (SJR). Pseudonoise (PN) codes can solve the sidelobe problem [16].

Some methods focus on the signal characteristics. It means that these methods concentrate on the differences between a real target signal and a DRFM repeat-back signal. A DRFM, as a device, has several limitations in its structure. These limitations, lead to some incompatibilities in the DRFM signal compared to a real scatter. Greco *et* al. [17], proposed a classification method based on a cone class. This method defines a classification problem based on the low digital-to-analog converter (DAC). The DAC number of quantization levels is low because the practical miniaturized DRFMs in airborne systems have low quantization levels. Furthermore, the sampling frequency is high to reach higher frequencies in the analog-to-digital (ADC) devices [17]. This method does not include the high quantities of jammer-to-signal ratio (JSR). Another method [18] concentrates on the signal pattern in time and frequency to discriminate the targets based on kernel linear discriminator analysis (KLDA) feature extraction. This method uses a support vector machine (SVM) for discrimination which requires more time for computation.

In most DRFM structures, the local oscillator (LO) is utilized to down-convert the transmitted radar signal and up-convert the simulated signal to radar frequency. These are several types of oscillators, including crystal oscillator, which is usually followed by a frequency multiplier, and voltage−controlled oscillator (VCO) in the phase−locked loop (PLL). The real physical oscillators have a random phase modulation named phase noise. Phase noise dispreads the signal spectrum. This makes the signal spectrum wider and spread to adjacent frequencies. This process can be modeled as a low−frequency flicker noise plus white noise [19].

Phase noise is one of the important problems in radio frequency (RF) systems as a result of imperfect oscillators [20]–[24]. Unlike white Gaussian noise, phase noise is residual and time varying. So, the power spectrum density (PSD) of phase noise has a significant status in RF systems. Phase noise is usually expressed as dBc/Hz. The effect of phase noise performance is considered at higher frequencies of carriers in radar systems [25]. The phase noise in RF signals or, equivalently, the jitter in time−based pulses influences the radar ability. Furthermore, all types of oscillators have their own phase noise characteristics that relate only to themselves. It can be written that the phase noise pattern of any oscillator is governed by its structure, which determines the PSD of phase noise and spurious frequency components.

In this paper, a novel anti-deception jamming method is proposed based on the phase noise difference of oscillators in received signals. In this technique, the transmitted CW radar signal is generated by a master oscillator (MO) with carrier frequency phase noise. It means that the transmitted signal is marked with slightly nonlinear frequency modulation produced by this oscillator. Obviously, the base station radars can use many kinds of sub-systems and devices in their systems. Therefore, they have low−phase noise oscillators, whereas the DRFM block does not have this advantage and the LO of the DRFM system has a high phase noise level. Furthermore, a simulated signal made through complex circuits including the mixer, analog filters, single−side band (SSB) modulator, digital signal processor (DSP), and/or field-programmable gate array (FPGA) have different PSD and higher phase noise levels in comparison to a real back-scatter one.

In other words, the phase noise level is increased when a signal is made through imperfect electronic devices. It can be considered very low phase noise MO and LO for carrier generation and down-conversion in radar systems. A system is provided to measure the phase noise of oscillators to investigate the phase noise spectrum of any kind of oscillators, which have their own patterns and power levels. Subsequently, P_D and P_{fa} are obtained for evaluating the performance of distinguishing real targets from false ones.

We consider different signal−to−noise ratios (SNR) and SJRs in predefined P_{fa}, and analyze P_D to verify the proposed method performance. The phase noise powers are measured through the same sets of circuits and coherent time periods. Then, the phase noise spectrum shape and its power can be used to recognize the real target back−scatter from the DRFM signal. Sometimes, control of the amplitude fluctuation of the received signal is very difficult, therefore, to quantify the phase noise of DRFM received signal with respect to the target signal, we present a different metric to compare phase noise levels that are normalized by signal power in predefined bandwidths. The likelihood ratio test (LRT) is used for target discrimination. In this case, a threshold level is achieved by minimum P_{fa} to discriminate the targets.

The proposed method has a simple structure based on the inherent characteristics of oscillators. It has no additional complexities and can easily be adapted to common radar systems. All presented results are investigated using real DRFM systems including sub-blocks in their structure.

We consider both L-band and X-band radar sensors with time delay and Doppler frequency in the presence of additive white Gaussian noise (AWGN). The results are shown for various cases including different ranges, Doppler frequencies, SNRs, and SJRs in both L-band and X-band.

The remainder of the article is organized as follows. Section II introduces the CW radar signal model with LFM modulation, and then considers the DRFM signal model. Section III explains the phase noise difference in an oscillator and a phase noise meter set-up, for measuring. Section IV describes the proposed method based on the different phase noise levels where DRFM has different oscillator types with its own phase noise PSD. Then, the theoretical verification is considered. Finally, a detector defined for target discrimination. In section V, the experimental implementations of DRFM are investigated in two radar bands (L-band and X-band) with their components. Then, the test results are shown in various conditions. In section VI, we present our conclusions.

II. SYSTEM MODEL

A. REAL TARGET SIGNAL

Nowadays, because of power limitation, most tracking radar systems are working in the CW mode with modulation. Tracking radar with linear frequency modulated continuous wave (LFMCW) signal assumes that a transmitted signal is infinite in time. Based on this assumption, the $s_t(t)$ radar transmitted signal can be described as

$$s(t) = \sqrt{E_s} e^{j(2\pi f_c t + \pi \mu t^2 + \varphi_0 + \varphi_{MO}(t))} \tag{1}$$

where E_s is the signal power, f_c describes the central MO frequency, μ is the chirp rate, φ_0 denotes the initial phase, and $\varphi_{MO}(t)$ is the instantaneous phase of the MO. The phase noise is a random process with unique PSD, $S_\varphi(f)$, and spectrum pattern. The received reflection signal from the target can be written as

$$r(t) = \sqrt{E_s}\tilde{a} e^{j(2\pi (f_c + f_{d_k})(t-\tau_k) + \pi \mu (t-\tau_k)^2 + \varphi_0 + \varphi_{MO}(t-\tau_k))} + n(t) \tag{2}$$

where f_{d_k} is Doppler frequency of moving target, and τ_k stands the time delay of the k^{th} detected target by research radar. The radar cross section (RCS) of target $\tilde{a}$ is the RCS with amplitude fluctuation, and $n(t)$ is the complex AWGN noise with zero mean and variance σ_0^2. Then, in a radar system, the received signal $r(t)$ is down-converted to f_{IF} intermediate frequency (IF) by mixing the received signal with LO signal. It can be defined as a multiplier, and the amplitude of the mixer output can be assumed as constant. The mixer output signal $y(t)$ is described as

$$y(t) = \sqrt{E_s}\tilde{a} e^{j(2\pi (f_{IF} + f_{d_k})t + \pi \mu t^2 - 2\pi \mu \tau_k t + \varphi_{MO}(t-\tau_k) - \varphi_{LO}(t))} + n_{IF}(t) \tag{3}$$

$$n_{IF}(t) = n(t) \times x_{LO}^*(t) \tag{4}$$

In (3), $n_{IF}(t)$ is the down-converted AWGN noise signal in the IF band and $x_{LO}^*(t)$ is the LO input signal of the mixer. After IF band−pass filter (BPF), the high−frequency components out of the filter pass band is neglected, and the effects of $e^{j(-2\pi (f_{IF} + f_{d_k})\tau_k + \pi \mu \tau_k^2 + \varphi_0)}$, conversion gain of mixer, and other losses are absorbed in $\tilde{a}$. If $r(t)$ signal is processed in the IF frequency, the BPF is used to suppress out−of−band components, noise, and other signal interference.

B. DRFM TARGET SIGNAL

The jammer is assumed to be self-protection (on board jammer) with $v_{r,J}$ relative radial velocity to radar. The DRFM captures the radar signal frequency and down−converts by mixer with its LO signal, and is then quantized by ADC [26]. Thus, the DRFM received signal $r_D(t)$ is

$$r_D(t) = \sqrt{E} a_j e^{j(2\pi (f_c + f_{r,J})(t-\tau_d) + \pi \mu (t-\tau_d)^2 + \varphi_0 + \varphi_{MO}(t-\tau_d))} + n(t) \tag{5}$$

where τ_d is the time delay between the radar and DRFM system proportional to distance, $f_{r,J}$ is the Doppler frequency related to jammer radial velocity, and a_j is the amplitude of the captured signal. Then, the signal is down-converted by the mixer to the IF frequency band. Therefore, we have

$$r_{IF}(t) = \sqrt{E} a_j e^{j(2\pi (f_{IF} + f_{r,J})t + \pi \mu t^2 + 2\pi \mu \tau_d t + \varphi_0 + \varphi_{MO}(t-\tau_d) - \varphi_{LO}^J(t))} + n_{IF}(t) \tag{6}$$

$\varphi_{LO}^J(t)$ is the instantaneous phase of the jammer LO, and $n_{IF}(t)$ is the band-limited noise in the IF band of the DRFM system. Finally, the simulated signal passes through reconstruction filter to minimize the effects of sampling frequency. Then, it up-converts by LO with $f_c + f_{d_J}$ frequency to send back to the hostile radar receiver. The relative velocity of the jammer is accounted for; therefore, f_{d_J} includes the $f_{r,J}$ (jammer velocity). The DRFM transmitted signal can be expressed as

$$s_J(t) = \sqrt{E_J}\tilde{a}_J e^{j(2\pi (f_c + f_{d_J})(t-\tau_f) + \pi \mu (t-\tau_f)^2)} \cdot e^{j(\varphi_{MO}(t-\tau_d-\tau_f) - \varphi_{LO}^J(t-\tau_f) + \varphi_{LO}^J(t))} \tag{7}$$

where E_J is the energy of the transmitted DRFM signal and $\tilde{a}_J$ denotes the RCS with the amplitude fluctuation of the false target. In a real target, the instantaneous amplitude of the echo signals is inverse proportional to the forth power of the target range and has fluctuations with propagation environment, the aspects view of the target structure and RCS of the target. The result of these parameters can be modeled by some stochastic processes [26]. In a DRFM system, the instantaneous amplitude ($\tilde{a}_J$) is produced by accounting the above parameters [26], [27]. f_{d_J} is the false target Doppler frequency. By accounting for the time delay between the DRFM and radar, τ_f is $\tau_J - \tau_{DL}$, which is related to the false simulated target range. Then, the received DRFM signal can be written as

$$r_J(t) = \sqrt{E_J}\tilde{a}_{r,J} e^{j(2\pi (f_c + f_{d_J})(t-\tau_J) + \pi \mu (t-\tau_J)^2)} \cdot e^{j(\varphi_{MO}(t-\tau_d-\tau_J) - \varphi_{LO}^J(t-\tau_f) + \varphi_{LO}^J(t))} + n(t) \tag{8}$$

where $n(t)$ is the AWGN part with zero mean and variance σ_0^2. The received signal amplitude is shown by $\tilde{a}_{r,J}$. Similar to the real target, the mixer output IF signal $y_J(t)$ at radar receiver can be described as

$$y_J(t) = \sqrt{E_J}\tilde{a}_J e^{j(2\pi(f_{IF}+f_{d_J})t+\pi\mu t^2-2\pi\mu\tau_J t)} \times e^{j(\varphi_{MO}(t-\tau_d-\tau_J)-\varphi_{LO}^J(t-\tau_f)+\varphi_{LO}^J(t-\tau_J)-\varphi_{LO}(t))} + n_{IF}(t) \quad (9)$$

where $\tilde{a}_J$ contains the effects of $e^{j(-2\pi(f_{IF}+f_{d_J})\tau_k+\pi\mu\tau_J^2+\varphi_0)}$, conversion gain of mixer, and other losses. The signal-to-noise ratio (SNR) of real target and DRFM are define as $E_s\sigma_{\tilde{a}}^2/\sigma_0^2$ and $E_J\sigma_{\tilde{a}_J}^2/\sigma_0^2$, respectively. Where $\sigma_{\tilde{a}}^2$ and $\sigma_{\tilde{a}_J}^2$ are the variances of the $\tilde{a}$ and $\tilde{a}_J$, and σ_0^2 is the thermal noise of receiver and AWGN of environment. In order to measure the phase noise of received signals, the antenna received signal is down-converted, then sampled before coming through the processing circuits in radar receiver system. It means the SNR is defined without processing gain.

III. PHASE NOISE MEASUREMENT AND DIFFERENCES

The phase noise measurement techniques can be sorted into direct spectrum analyzer read out, two-oscillator method, and single oscillator method [28]–[31]. The direct spectrum analyzer is easy operation and be used for general phase noise measurement. The performance limitations of this method are residual FM of spectrum analyzer internal LO, the additional phase noise of LO, mixing up the effects of the amplitude noise and phase noise, the noise figure (NF) of analyzer raises the measured phase noise read out [29].

Another method is the reference source with phase detector that measures the residual additive noise for two oscillators and has lower phase noise floor [28], [29]. However, this method requires a very clean and automatically tunable reference oscillator with high drift ability in wide band that is so hard to implement [29]. Using the two channels cross-correlation method attains better measuring performance, but, the measuring action speed depends on the number of correlations. In radar system, the phase noise measurement needs numerous numbers of correlations that is impassible with this method [30].

Finally, the single oscillator method like Frequency discriminator is a simple technique that utilized for phase noise measurement of all kinds of oscillators. This method is applicable especially when the signal source has low rate phase noise, and spurious frequencies in sideband. Furthermore, the amplitude noise can be removed by using limiting amplifier and phase detector. A greater time delay improves the discriminator lower frequency characteristics, however, it needs longer length which increases the loss of the delay line and decreases the maximum offset frequency measuring. In practice, the maximum offset frequency is not important for phase noise measurement of radar system. This technique is best for low phase noise signals without using of additional signal source with undetermined level of phase noise [28], [31].

A. PHASE NOISE MEASUREMENT

In this section, the power spectrum of the radar transmitted signal is approximately measured by a simple method. To measure the phase noise of an oscillator output signal, several methods can be used such as an additional oscillator, mixer, and spectrum analyzer [28]. The block diagram of the used phase noise measurement set-up is shown in Fig. 1.

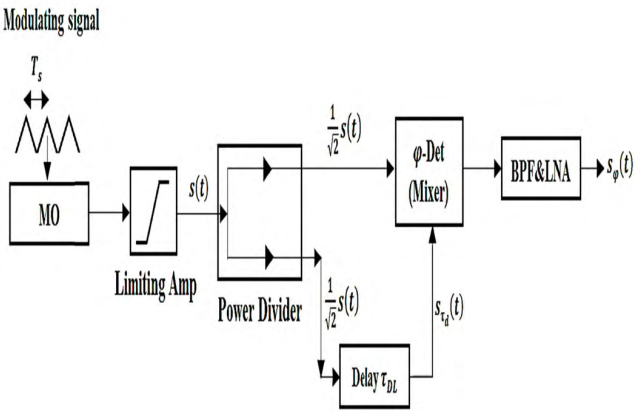

FIGURE 1. Block diagram of a phase noise measurement set-up.

In this paper, to avoid the effects of additional phase noise produced by an external oscillator, a single delay line and a low noise mixer act as a frequency demodulator [28]. The oscillator signal with LFM modulation can be expressed as

$$s(t) = A_{os}e^{j(2\pi f_c t+\pi\mu t^2+\varphi_0+\varphi_{os}(t))} \quad (10)$$

A_{os} denotes the amplitude of the oscillator signal, f_c is the oscillator carrier frequency, φ_0 denotes the initial phase, and $\varphi_{os}(t)$ stands the instantaneous phase of the oscillator. Then, the oscillator signal is divided into two similar signals by using a power divider; one goes through a delay line with an appropriate length and connected to the RF port of mixer, and another acts as the LO signal for mixer. The amplitude of the input signal becomes limited to minimize the effect of amplitude noise and fluctuations. A BPF with a specified bandwidth suppresses the out−of−band components and the low noise amplifier (LNA) amplifies the mixer output with a low noise figure. Therefore, the output of filter can be expressed as

$$s_\varphi(t) = A_{os}e^{j(2\pi f_c\tau_d+\varphi_{os}(t)-\varphi_{os}(t-\tau_d))} \quad (11)$$

where τ_d is the time delay of the delay line. It can be assumed that $\delta\varphi_{os}(t,\tau_{DL}) = \varphi_{os}(t) - \varphi_{os}(t-\tau_{DL})$. Here $\delta\varphi_{os}(t,\tau_{DL})$ denotes the phase noise term. If τ_{DL} is chosen by these two conditions $\tau_{DL} \ll T_M$, and the maximum frequency of phase noise measurement $f_{max} \ll 1/\tau_{DL}$, where T_M is the time period of frequency modulated signal or time of frequency sweep. By this assumption, phase change during the time for LFM is very slow compared to rapid random phase noise changing. Therefore, the total phase noise change is not affected by the LFM. Hence, based on above-mentioned condition, and for actual oscillators $\delta\varphi_{os}(t,\tau) \ll 1$, the $\varphi_{os}(t)$

process can be simplified on the interval of the length τ. Therefore, it can be written as

$$\delta\varphi_{os}(t,\tau) \approx \tau \frac{d\varphi_{os}(t)}{dt} \tag{12}$$

Therefore, by substituting (12) in (11), the BPF output signal is

$$s_{\varphi}(t) = A_{LNA}\left(1 + j\tau_{DL}\frac{d\varphi_{os}(t)}{dt}\right)e^{j2\pi f_c \tau_{DL}} \tag{13}$$

It can be seen that the phase noise power is proportional to the time delay for small τ_{DL}. The very low frequencies and DC component are eliminated by the BPF in Fig. 1. The PSD of this filtered signal is proportional to the phase noise of the oscillator $S_{\varphi_{os}}(f)$ that can be taken from

$$S_{s_{\varphi}}(f) = A_{LNA}^2 \tau_d^2 S_{\frac{d\varphi_{os}(t)}{dt}}(f) \tag{14}$$

Furthermore, the PSD of the $\frac{d\varphi_{os}(t)}{dt}$ is $S_{\frac{d\varphi_{os}(t)}{dt}}(f) = 4\pi^2 f^2 S_{\varphi_{os}}(f)$; so, the final PSD of the phase noise can be written as

$$S_{s_{\varphi}}(f) = 4\pi^2 A_{os}^2 \tau_d^2 f^2 S_{\varphi_{os}}(f) \tag{15}$$

It seems that based on real conditions for radar systems, the effect of LFM is not apparent. The phase noise power in the determined $BW = f_{max} - f_{min}$, $P_{s_{\varphi}}$, can be defined as

$$P_{s_{\varphi}} = 4\pi^2 A_{os}^2 \tau_d^2 \int_{f_{min}}^{f_{max}} f^2 S_{\varphi_{os}}(f)\, df \tag{16}$$

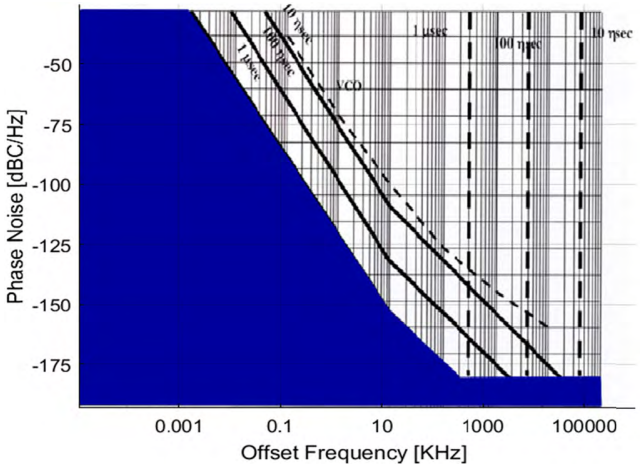

FIGURE 2. Effect of delay time on the noise floor [32].

where f_{min} and f_{max} are the minimum and maximum frequency of BPF, respectively. In this paper, a practical phase noise measurement set-up is provided to measure and compare the phase noise of various oscillator signals by using the same measure set-up. Fig. 2 shows the effect of different amount of τ_d. It can be seen greater the time delay τ_d improves the noise floor and total power of phase noise components is increased. On the other side, greater τ_d increase power loss in the delay-line and limit the maximum offset frequency f_{max}. It will exceed the source power available and cancel further improvement [32].

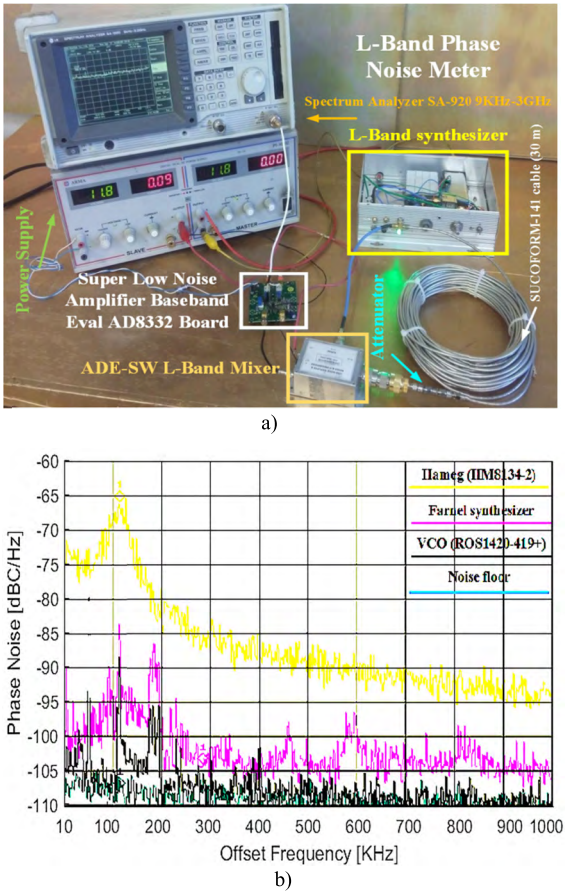

FIGURE 3. a) An experimental phase noise meter for L-band. b) Measured PSD of phase noise for the some types of L-band signal source.

B. PRACTICAL PHASE NOISE MEASUREMENTS

Several practical tests are provided to show the power and spectrum pattern differences of phase noise for various signal sources. Fig. 3 a) shows the phase noise meter implementation for the L-band frequency. The implementation set-up is taken from the previous section. This process measures the phase noise PSD with accurate approximation, but the phase noise term still depends on τ_{DL} and frequency. To measure the phase noise in the (10 kHz, 1 MHz) band, an appropriate time delay ($\tau_{DL} = 150$ nano-seconds) is selected. It means the $f_{max} = 1/2\pi\tau_{DL} \approx 1MHz$. In the L-band, the phase noise meter set-up includes a power divider, a succuform-141 coaxial cable with 30 meters length, and an ADE-SW mixer chip, and the output of mixer is amplified by a super LNA eval AD8332 board. The spectrum of the amplified signal is shown by the LG SA-920 (9 kHz-3 GHz) spectrum analyzer. The set-up of the phase noise floor is approximately -110 dBC/Hz. Some signal sources that are tested by this set-up are shown in Table I. In Fig. 3 b); it can be seen that any practical signal sources have their own phase noise characteristics and detected phase noise signal PSD in dBC/Hz versus offset frequencies. In L-band results, the used VCO (ROS-1420-419+) has a very low phase noise power

TABLE 1. L-band signal sources.

X-band	
Signal source	***Company***
VCO (ROS_1420_419+)	Mini-circuits
HAMEG (HM81342_ synthesizer)	HAMEG
Farnel PSG 1000	Farnel

TABLE 2. X-band signal sources.

X-band	
Signal source	***Company***
MKU 10 BAKE	Kuhne electronic
HMC778 (Fractional-N PLL)	Hittite Microwave Corporation
VCO (ROS_3000v_819+) & Freq. Multiplier × 4 (MKU XN 10 TX)	Mini-circuits & Kuhne electronic

level. This oscillator approximately reaches the noise floor of the set-up noise in higher frequencies; however, in lower frequencies it has several powerful components. Its average phase noise power differs from the noise floor level measuring setup at least 2-3 dB. The model HM81342 HAMEG synthesizer has an extremely high phase noise level with a distinctive pattern. This advantage means a distinctive power and pattern for any signal sources that can be considered as target discrimination basis. It has a minimum of 20 dB greater average power to the noise floor.

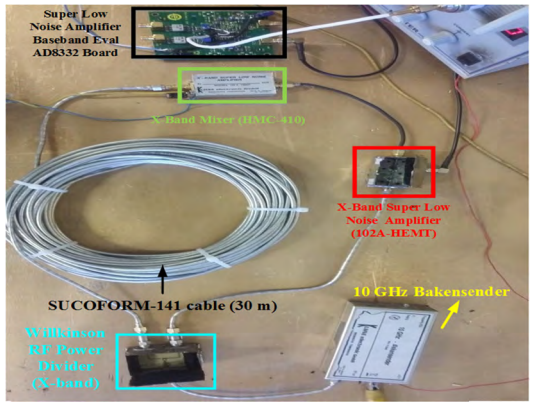

a)

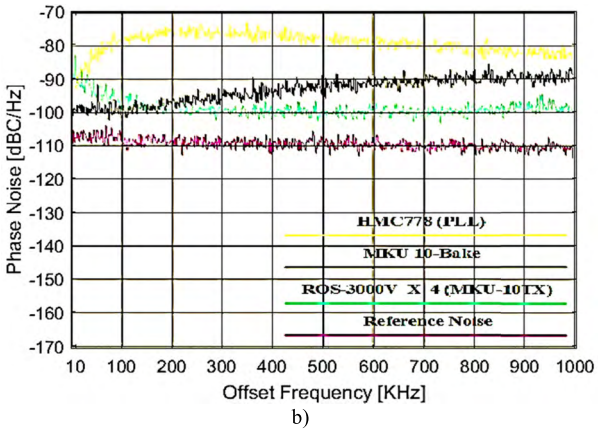

b)

FIGURE 4. a) An experimental phase noise meter for X-band, b) Measured PSD of phase noise [dBC/Hz] versus offset frequencies for the some types of X-band signal source.

Finally, the Farnel synthesizer has a medium phase noise power in comparison to the above-mentioned signal sources and has approximately 5-6 dB phase noise power difference.

In the X-band, Fig. 4 a) shows an X-band Wilkinson RF power divider for dividing RF power, a succuform-141 coaxial cable with 30 meters length, and a Hittite-HMC410 mixer, and the output of the mixer is amplified by a super LNA eval AD8332 board. The amplified signal is shown by an LG SA-920 (9 kHz-3 GHz) spectrum analyzer. The noise floor of the used set-up is approximately -110 dBC/Hz. The signal sources that are tested using the above-mentioned setup (shown in Table 2). To prevent the effect of the amplitude variations, all input powers to the phase noise meter are equal. Fig. 4 b) shows the phase noise PSD of detected signals in dBC/Hz for three practical X-band signal sources versus offset frequencies. The MKU 10 BAKE oscillator has a completely different phase noise pattern. The PSD of this source has low power in low frequencies, and this increased as the frequency increased. It has 13dB higher phase noise power in comparison with the noise floor. The source made by Hittite -HMC778 (PLL) has high phase noise with individual patterns. At least, it has a 30 dB greater average power than the noise floor. In the third measurement, VCO in the S-band is frequency multiplied by using an MKU XN ×4 block to X-band, and has a different phase noise power. It gives approximately 12 dB higher average power than the set-up thermal noise floor.

IV. THE PROPOSED METHOD

The proposed anti-deception method is based on phase noise different characteristics of signal sources in received

signals. We assumed that the transmitted CW radar signal with LFM is generated by an MO oscillator. Fig. 5 shows the block diagram of the proposed method with a real target signal and a false target produced by the DRFM system. MO has a low phase noise power level with a specific PSD pattern.

The base station radars can use many kinds of sub-systems and devices in their systems. In this method, the radar systems use low phase noise devices, whereas the DRFM system does not have this advantage and the LO oscillator in the DRFM system has different phase noise distribution and power level. Additionally, a simulated signal is made through some different electronic devices with its own frequency response. The DRFM system contains a mixer, analog filters, single−side band (SSB) modulator, a digital signal processor (DSP), and/or field-programmable gate array (FPGA), ADC, and DAC blocks.

These devices change the radar signal PSD and produce

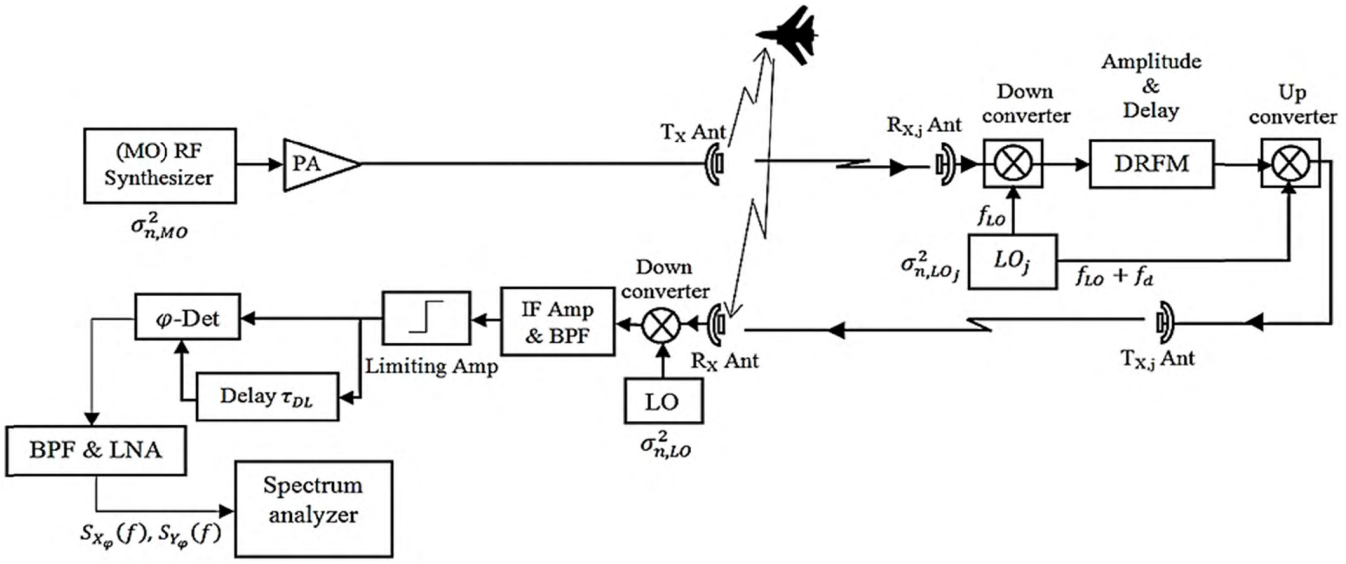

FIGURE 5. Block diagram of proposed method to measure the phase noise of target signals.

higher phase noise level. In comparison to the DRFM signal, the hostile radar receiver has lower phase noise level. In addition, in many DRFM systems at the last stage, the signal is up-converted by a jammer second LO. The above-mentioned effects change the DRFM signal PSD and make higher phase noise power in comparison to a real back-scatter one. Based on (6) and (9), the received signal from real target and DRFM target in the IF band can be represented by

$$y_\varphi(t) = \begin{cases} \sqrt{E_s}\tilde{a}_r e^{j\left(2\pi\left(f_{IF}+f_{d_k}\right)t+\pi\mu t^2+2\pi\mu\tau_k t\right)}. \\ e^{j\left(\varphi_{MO}(t-\tau_k)-\varphi^r_{LO}(t)\right)} + n_{IF}(t) : \text{RealTarget} \\ \sqrt{E_J}\tilde{a}_J e^{j\left(2\pi\left(f_{IF}+f_{d_J}\right)t+\pi\mu t^2+2\pi\mu\tau_J t\right)}. \\ e^{j\left(\varphi_{MO}(t-\tau_{DL}-\tau_J)-\varphi^J_{LO}(t-\tau_f)+\varphi^J_{LO}(t-\tau_J)-\varphi_{LO}(t)\right)} \\ \qquad + n_{IF}(t) : \text{DRFM} \end{cases} \tag{17}$$

By assuming that $\delta\varphi_{os}(t,\tau) \ll 1$, the IF filter can suppress the out−of−band components and then amplify the phase noise term. The terms $\mu\tau_k$ and $\mu\tau_J$ are absorbed in Doppler frequency f_{d_k} and f_{d_J}. Therefore in the radar receiver, we have

$$y_\varphi(t) = \begin{cases} \sqrt{E_s}\tilde{a}_r\left(1+j\left(\tau_k\delta\varphi_r(t,\tau_k)+\pi\mu t^2\right)\right) \\ \qquad \cdot e^{j\left(2\pi\left(f_{IF}+f_{d_k}\right)t\right)} + n_{IF}(t) : \text{RealTarget} \\ \sqrt{E_J}\tilde{a}_J\left(1+j\tau_{J,f}\left(\delta\varphi^J_r(t,\tau_{DL}+\tau_J)\right.\right. \\ \qquad \left.\left.+\delta\varphi^J_{LO}\left(t,\tau_{J,f}\right)+\pi\mu t^2\right)\right) \\ \qquad e^{j\left(2\pi\left(f_{IF}+f_{d_J}\right)t\right)} + n_{IF}(t) : \text{DRFM} \end{cases} \tag{18}$$

where $\delta\varphi_r(t,\tau_k) = \varphi_{MO}(t-\tau_k) - \varphi^r_{LO}(t)$ belongs to the real target, and the total jammer phase noise is $\delta\varphi_J(t,\tau_{J,f}) = \delta\varphi^J_r(t,\tau_{DL}+\tau_J) + \delta\varphi^J_{LO}(t,\tau_f-\tau_J)$, whereas $\delta\varphi^J_r(t,\tau_{DL}+\tau_J) = \varphi_{MO}(t-\tau_{DL}-\tau_J) - \varphi^r_{LO}(t)$ relates to the radar phase noise.$\delta\varphi^J_{LO}(t,\tau_f-\tau_J) = \varphi^J_{LO}(t-\tau_J) - \varphi^J_{LO}(t-\tau_f)$ is the instantaneous phase of DRFM LO in $t=\tau_J$ and $t=\tau_f$ for up-converting and down-converting, respectively. Eq. (18) is achieved for LFMCW received signal, and this relation is changed for other kinds of FMCW signals.

Finally at the output of phase noise measuring setup the IF components (IF plus Doppler frequency) are removed by a BPF, and assuming that $n_{IF}(t)$ is AWGN noise and these phase noises are independent. Therefore, these terms are replaced by their expectation values. Finally, the power spectrum of phase noise $S_{Y_\varphi}(f)$ is

$$S_{Y_\varphi}(f) = \begin{cases} E_s\left|\tilde{a}_r\right|^2\left(\tau_k^2 S_{\frac{d\varphi_r(t,\tau_k)}{dt}}(f) + \frac{4\pi^2\mu^2}{(2\pi f)^6}\right) \\ \qquad + N_{IF}(f) : \text{RealTarget} \\ E_J\left|\tilde{a}_J\right|^2\left(\left(\tau_{DL}+\tau_J\right)^2 S_{\frac{d\varphi^J_r(t,\tau_d+\tau_J)}{dt}}(f)\right. \\ \qquad \left.+\tau^2_{J,f} S_{\frac{d\varphi_J(t,\tau_{J,f})}{dt}}(f) + \frac{4\pi^2\mu^2}{(2\pi f)^6}\right) \\ \qquad + N_{IF}(f) : \text{DRFM} \end{cases} \tag{19}$$

In (19), the term $\frac{4\pi^2\mu^2}{(2\pi f)^6}$ appear in both real target and DRFM signal, although due to the dominant f^6 term in $\frac{4\pi^2\mu^2}{(2\pi f)^6}$, it has very small quantity in phase noise measuring band (10 kHz, 1 MHz) and can be neglected. The $N_{IF}(f)$ is assumed as the Gaussian PSD of the filtered AWGN noise power spectrum. Based on the relation $S_{\frac{d\varphi(t)}{dt}} = 4\pi^2 f^2 S_\varphi(f)$, the final PSD of $S_{Y_\varphi}(f)$ can be written as

$$S_{Y_\varphi}(f) = \begin{cases} 4\pi^2 E_s\left|\tilde{a}_r\right|^2 f^2 \tau_k^2 S_{\varphi_r(t,\tau_k)}(f) + N_{IF}(f) : \text{RealTarget} \\ 4\pi^2 E_J\left|\tilde{a}_J\right|^2 f^2\left(\left(\tau_{DL}+\tau_J\right)^2 S_{\varphi_r(t,\tau_d+\tau_J)}(f)\right. \\ \qquad \left.+\tau^2_{J,f} S_{\varphi_J(t,\tau_{J,f})}(f)\right) + N_{IF}(f) : \text{DRFM} \end{cases} \tag{20}$$

Finally, the phase noise power in the measuring bandwidth BW, P_{Y_φ}, can be written as

$$P_{Y_\varphi} = \begin{cases} 4\pi^2 E_s \left|\tilde{a}_r\right|^2 \tau_k^2 \int_{f_{min}}^{f_{max}} f^2 S_{\varphi_r(t,\tau_k)}(f)\, df + N_W \\ 4\pi^2 E_J \left|\tilde{a}_J\right|^2 \int_{f_{min}}^{f_{max}} f^2 \\ \quad \times \left(\begin{array}{l} (\tau_{DL}+\tau_J)^2 S_{\varphi_r(t,\tau_{DL}+\tau_J)}(f) \\ +\tau_{J,f}^2 S_{\varphi_J(t,\tau_{J,f})}\left(f, \tau_{J,f}\right) \end{array} \right) df + N_W \end{cases} \quad (21)$$

where $N_W = \int_{f_{min}}^{f_{max}} N_{IF}(f)\, df \approx BW \frac{N_0}{2}$ is the noise power that appears in the measuring bandwidth. The dynamic range of the received signal is very high and the variation of its amplitude cannot be eliminated by the limiting amplifier; for weak signals, hence, in particular, this causes some errors in phase noise measurement. Therefore, a practical metric is introduced to quantify the normalized phase noise difference between the received signal with respect to the total phase noise of MO and LO in the radar system. ρ_{S_φ} is the phase noise Euclidean distance power that is normalized by the product of radar phase noise and received signal phase noise.

$$\rho_{S_\varphi} = \frac{\int_{f_{min}}^{f_{max}} \left|S_{Y_\varphi}(f) - S_{X_\varphi}(f)\right|^2 df}{\int \left|S_{Y_\varphi}(f)\right| df \int \left|S_{X_\varphi}(f)\right| df} \quad (22)$$

where $S_{X_\varphi}(f)$ is the phase noise power spectrum of the signal source of the radar that is measured by the same method. In (22), the normalized Euclidean distance for real target and DRFM target power spectrums becomes the basis of the discrimination procedure. The spectrum analyzer measures the noise power of the input signal in the desired frequency range (f_{min}, f_{max}). Then, $S_{X_\varphi}(f)$ and $S_{Y_\varphi}(f)$ versus frequency is measured using the spectrum analyzer. According to (22), ρ_{S_φ} can be calculated directly. More simplicity can be achieved by use of Cauchy–Schwarz inequality. Note that $S_{Y_\varphi}(f)$, $S_{X_\varphi}(f) \geq 0$ are real quantities, note also that

$$\int_{f_{min}}^{f_{max}} \left(S_{Y_\varphi}(f) - S_{X_\varphi}(f)\right)^2 df \leq \left(\int_{f_{min}}^{f_{max}} \left|S_{Y_\varphi}(f) - S_{X_\varphi}(f)\right| df\right)^2 \quad (23)$$

By substituting (23) in (22), the upper band of ρ_{S_φ} can be written as,

$$\rho_{S_\varphi} \leq \frac{\left(\int_{f_{min}}^{f_{max}} S_{X_\varphi}(f)\, df\right)^2 + \left(\int_{f_{min}}^{f_{max}} S_{Y_\varphi}(f)\, df\right)^2}{\int_{f_{min}}^{f_{max}} S_{X_\varphi}(f)\, df \int_{f_{min}}^{f_{max}} S_{Y_\varphi}(f)\, df} - 2 \quad (24)$$

Based on (24), if the normalized Euclidean distance (ρ_{S_φ}) between two signals is less than the threshold level, it is detected as a real target; otherwise, it is considered a jammer signal. Eq. (24) can be calculated by simply using the measured phase noise power (via the spectrum analyzer). In the tracking radar systems, the antenna beam is pointed on the target position; hence, the received signal of clutter is weaker than search radar system with fan beam that receives the ground clutter strongly. Furthermore, the dynamic range of RF front-end block in radar receiver and the proposed phase noise meter is high enough to prevent nonlinearity effects like intermodulation.

In operational tracking radar system after locking on the target, the first important step is evaluating the reality of target. Based on the mentioned assumptions, the proposed method can discriminate the real target from DRFM target. Usually, a DRFM (on board jammer) produces some powerful false targets with different ranges and velocities in order to deceive the radar receiver. If two received signals have enough Doppler frequency distance, each of them can be seen as a separate target and the recognition process can be repeated. Otherwise, if two target signals have the same Doppler frequency and range. In this rarely case, this method detects the signal as a DRFM target without any other detected real target in the antenna beam coverage which gives information about artificial character of this target that can lead the decision unit to track on jammer (TOJ) state for this on board jammer.

V. EXPERIMENTAL RESULTS

In this section, we present experimental results of implementation in order to evaluate the proposed method. All presented results are achieved in two operational bands (L-band, X-band) of radar systems. This section has two subsections. In the first subsection, the experimental set-up is investigated and particular aspects of the implementations are discussed. In the second, the experimental results are analyzed with details.

A. EXPERIMENTAL SET-UP

We present two experimental results of DRFM systems to analyze the performance of the proposed method in Fig. 5. For L-band tests, the carrier frequency is 1.3045 GHz, and the LFM frequency deviation is 200 kHz with a sweep rate 40 Hz. The power of radar transmitter is 1.8 KW, Tx and Rx antennas gain are approximately 33 dB, the front-end block gain 22 dB, and the radar receiver total noise figure (NF) plus other microwave components losses is around 2 dB.

Total tests in this band are done with the same low phase noise VCO (ROS-1420-419+) which is controlled by PLL for both radar and DRFM systems. In this setup, DRFM received the radar signal, which was first enriched by a low−noise RF amplifier that contains PGA-103^+ with high dynamic range (IP3 = 45 dBm at 1 GHz), and low NF (NF = 0.6 dB at 1GHz). The mixer ADE−5W (Mini circuits) is used in this band, which is followed by BPF and a low noise MMIC (MAR-6) as IF amplifier. Then, it goes through the RF switch to the L-band down-converter.

The IF output proceeds to ADC with 10 quantization bits, then the digital signal is processed by SPARTAN III FPGA to produce the desirable time delay and amplitude. The processed signal is then converted to an analog signal by DAC with 12 quantization bits. The output of DAC is filtered by IF BPF (reconstruction filter) to reduce the effects

of sampling. The analog SSB modulator produces the desired local frequency plus Doppler frequency ($f_{LO} + f_d$) by two quadrature signals. The Doppler frequency signals are produced by a programmed micro-controller. The output of the SSB modulator is mixed by the IF signal and up-converts to the L-band.

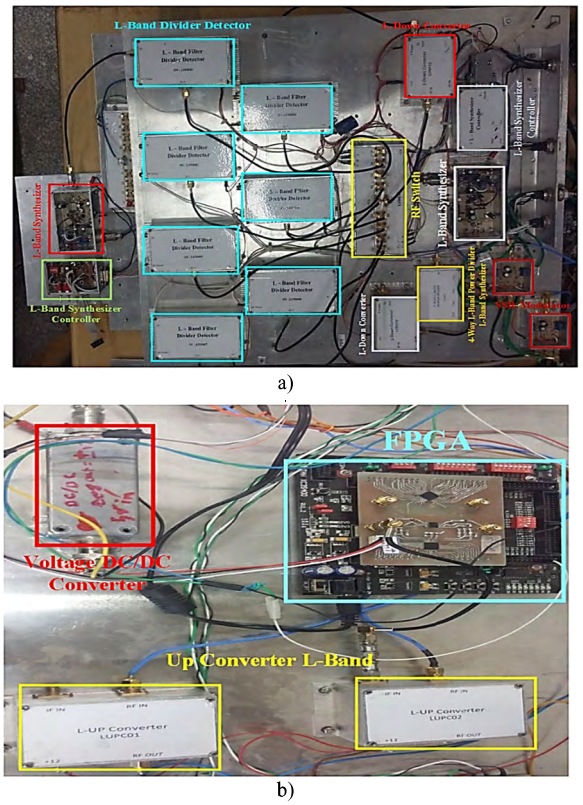

FIGURE 6. Experimental DRFM mounted on two plates in L-band. a) Left plate contains RF blocks, b) Right plate contains digital devices.

This signal is then amplified and sent-back to the hostile radar. Fig. 6 shows the DRFM set-up for L-band mounted on two plates. Fig. 6 a) shows the RF components of DRFM and Fig. 6 b) represents the digital devices besides the L-band up-converter. In X-band tests, the carrier frequency is 10.2454 GHz, and the LFM frequency deviation is 200 kHz with a sweep rate 40 Hz. The power of radar transmitter is 1.5 KW, Tx and Rx antennas gain are approximately 35 dB, the front-end block gain 24 dB, and the radar receiver total noise figure (NF) plus other microwave components is around 6 dB. Naturally, the phase noise power in the X-band is higher than that in the L-band. Unlike L-band tests, X-band tests are done with different oscillators. The radar oscillator is a crystal oscillator (MKU 10 BAKE) with very low phase noise level. However, the DRFM uses an S-band VCO (ROS-2960), which is multiplied by a MKU XN $\times 4$ to X-band and controlled by a PLL. In this set-up, DRFM receives the radar signal and strengthens signal via the RF amplifier that contains AVA$-$183A with high dynamic range (IP3 $=$ 28 dBm at 10 GHz) and NF is 4.5 dB. The mixer

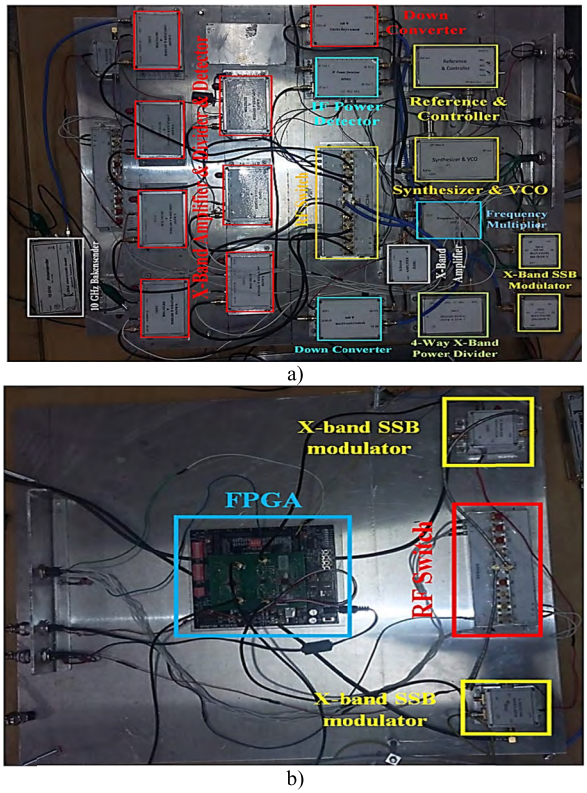

FIGURE 7. Experimental DRFM mounted on two plates in X-band. a) Left plate contains RF blocks, b) Right plate contains digital devices.

HMC$-$410 (Mini circuits) is used in this band, which is followed by BPF and a low noise MMIC (MAR-6) as IF amplifier. Then, the RF switch output is down-converted to IF frequency. The IF output proceeds to ADC with 10 quantization bits, and processed by SPARTAN III FPGA to create desirable range (delay) and amplitude. The processed signal is converted to analog signal by DAC with 12 quantization bits. The output of DAC is filtered by IF reconstruction filters to reduce the effects of sampling. The analog SSB modulator produces the desired local frequency plus Doppler frequency ($f_{LO} + f_d$) by two quadrature signal. The Doppler frequency signals are produced by a programmed micro-controller. The output of the SSB modulator is mixed by the IF signal and up-converts to the X-band. This signal is amplified and sent-back to the hostile radar. Fig. 7 shows the DRFM set-up for an X-band mounted on two plates. Fig. 7 a) shows the RF components of DRFM and Fig. 7 b) represents the digital devices besides the X-band up-converter.

The major kinds of tracking radars work in microwave bands like L, S, C, X, and Ku band that in these bands the environment noise is less than high frequency (HF), and very high frequency (VHF) bands. In these mentioned bands, the radar tracks only targets with high SNRs. In these conditions, the environment noise is smaller than the radar receiver thermal noise. The thermal noise (flat white noise) from radar receiver devices, and flicker noise from LNA and RF amplifiers increase the noise floor measurement [33]. The flicker noise

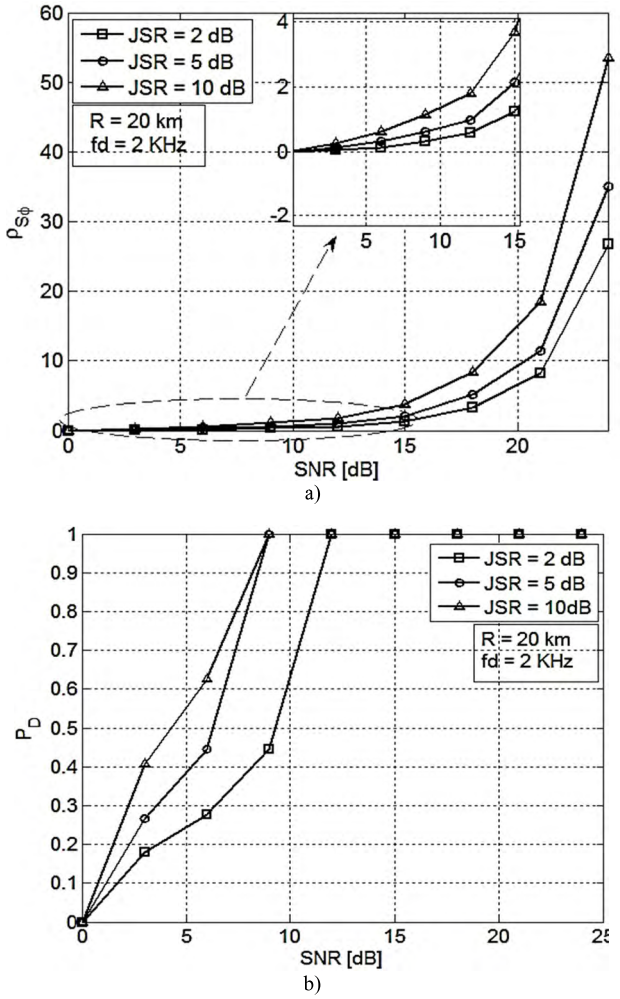

FIGURE 8. a) The ρ_{S_φ} in L-band for different SNRs. b) Probability of detection P_D for various SNRs in the case of very low false alarm.

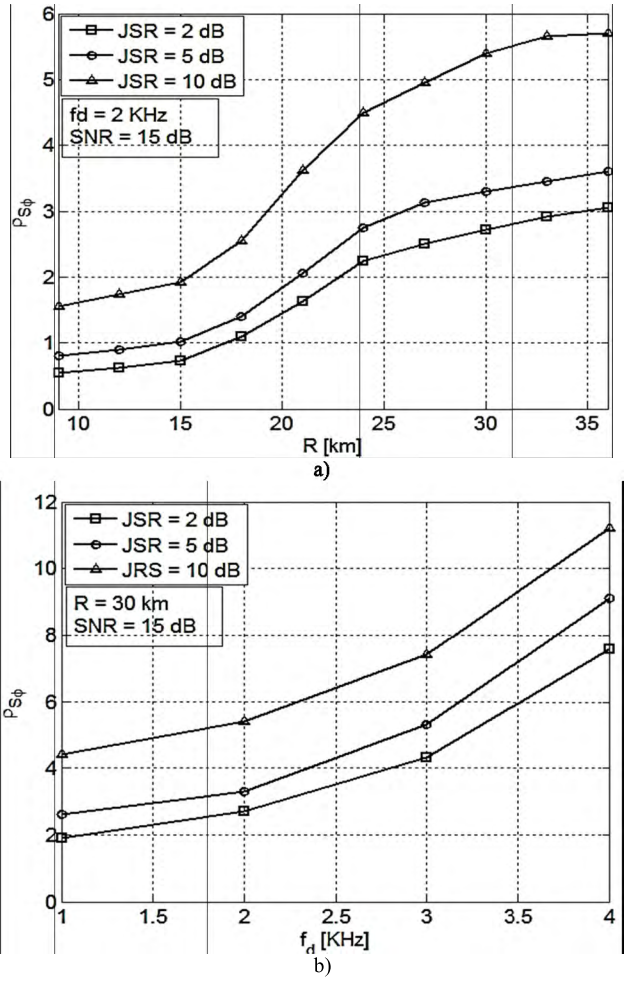

FIGURE 9. a) ρ_{S_φ} for DRFM target in L-band versus range. b) ρ_{S_φ} for DRFM target versus Doppler frequency.

approaches to the thermal noise at higher offset frequencies. The phase noise of oscillators in microwave bands is very greater than thermal noise of first stage of RF amplifiers or LNA as in [33]–[35]. Furthermore, the phase detector in frequency discriminator canceled the amplitude noise of thermal noise which suppresses the thermal noise effect. The thermal noise and NF of devices are uncorrelated to phase noise [31]. Generally, a practical oscillator of radar system has very low phase noise. However, when a signal is down/up-converted (mixer and LO) and amplified by RF amplifier besides the effect of DRFM jitter on sampling error and quantization error in ADC [17], [36], [37]. The final phase noise of DRFM signal is increased and changed, clearly. Finally, it should be mentioned that any noise floor level is directly related to input signal PSD that enters to phase noise measurement equipment.

B. EXPERIMENTAL RESULTS

In this section, the LFMCW radar is considered in L-band with 1.3045 GHz carrier frequency. For phase noise measurement, the duration of the received signal is 2 seconds. All targets are approaching at a determined range. It is fairly obvious when the tracking radar has locked onto the target. The SNR is large enough and the amplitude fluctuation and target RCS variation are using a slow model. Therefore, the limiting amplifier eliminates amplitude variation. The received signals are down-converted with the L-band mixer, and then filtered in band 10 KHz−1 MHz. The amplified filtered signals are used for measuring the phase noise power in a determined frequency range using the spectrum analyzer. The operational range cells are between 9 km−40 km. The maximum delay time for processing and decision is 2 seconds. All experimental results are based on 20 independent tests. A DRFM false target are considered in 20 km range and the radial velocity is approximately 0.7 Mach ($f_d = 2$ KHz). Fig. 8 a) shows ρ_{S_φ} versus various SNRs when JSR = 2, 5, 10 dB. It can be seen for SNR > 10 dB, ρ_{S_φ} increases by AWGN noise effect reduction, although increasing the JSR makes the discrimination better. P_D represents the probability of true discrimination of the real target from the jammer. In practical case, when $0 \leq \rho_{S_\varphi} \leq 0.5$, the detected target assumes to be real target.

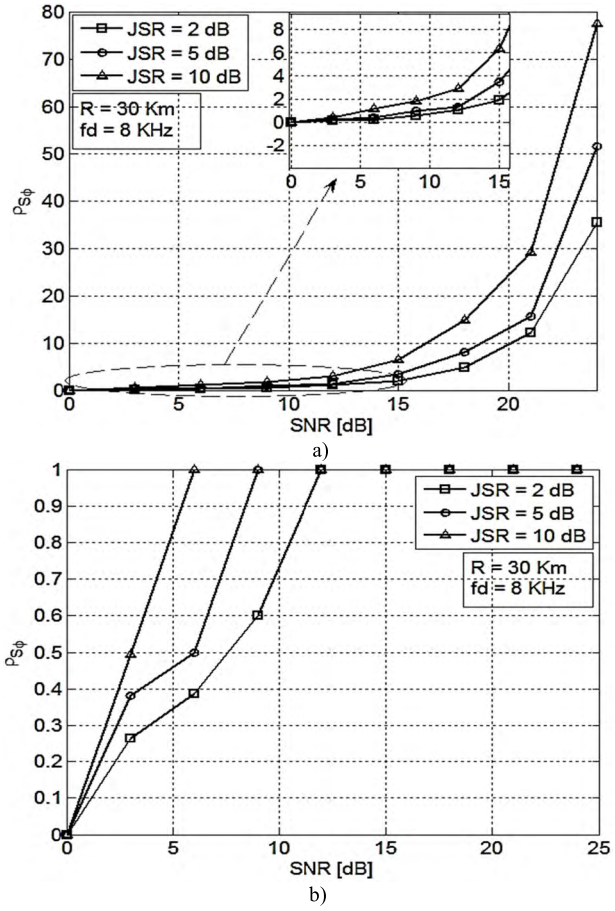

FIGURE 10. a) The ρ_{S_φ} in X-band for different SNRs. b) Probability of detection P_D for various SNRs in the case of very low false alarm.

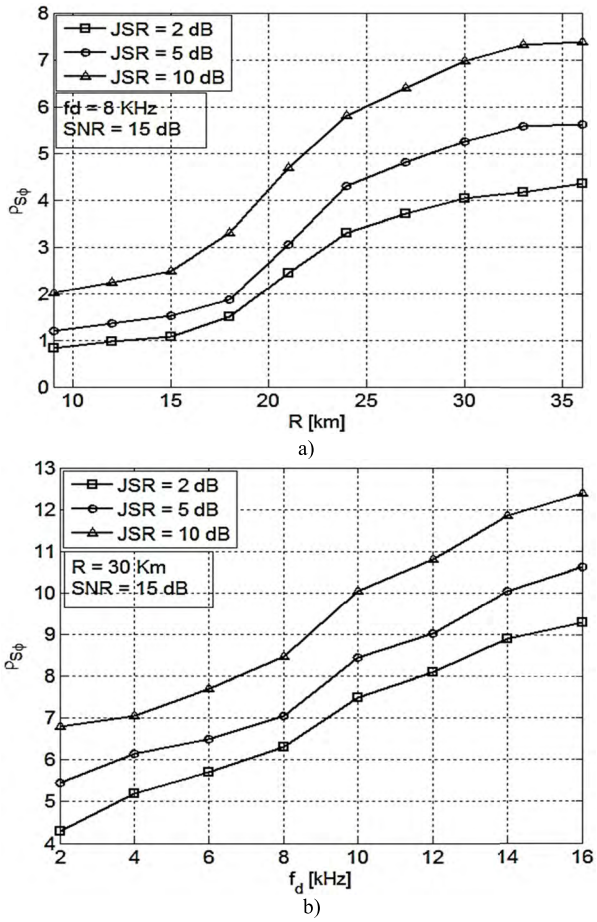

FIGURE 11. a) The ρ_{S_φ} for DRFM target in X-band versus ranges. b) The ρ_{S_φ} for DRFM target versus Doppler frequency.

On the other hand, when $\rho_{S_\varphi} \geq 1$, the tracking target assumes as DRFM target. $0.5 < \rho_{S_\varphi} < 1$ is the ambiguity area of detection. Fig. 8 b) shows the $P_D$based on different SNR. Based on the results, accurate detection ($P_D > 90$ %) is achieved when SNR > 10 dB. The Fig. 9 a) displays the ρ_{S_φ} of the received signal phase noise versus different time delays (ranges), where the Doppler frequency of the target is 2 KHz, and the SNR is approximately 15 dB. It can be seen that ρ_{S_φ} for the DRFM signal in $R \geq 18$ km is greater than the threshold level for all assumed ranges when JSR = 2, 5, 10 dB. Furthermore, the phase noise power increases in higher ranges. This happens because of the increased time−delay between the DRFM signal and the reference radar signal, which generates more low−frequency phase noise. Fig. 9 b) reveals the ρ_{S_φ} variation versus target speeds in 30 km range and SNR is 15 dB.

Consequently, the proposed method can detect all jammer signals in various situations with a P_D of more than 90%.

In the X-band radar system, generally the phase noise power is greater than that in the L-band. In this test, the carrier frequency is 10.2454 GHz. The received signals are down-converted with the X-band mixer and filtered by BPF limited to 10 kHz−1 MHz for calculating the phase noise power.

Similarly, the operational range cells are between 9Km − 40 Km. The maximum period for processing and decision is 2 seconds. All experimental results are based on 20 independent tests. Similar to L-band results, when $0 \leq \rho_{S_\varphi} \leq 0.5$, the detected target assumes to be a real target and $\rho_{S_\varphi} \geq 1$ the tracking target assumes as a DRFM target.

A DRFM false target is considered in 30 Km range and the Doppler frequency $f_d = 8$ KHz (Fig. 10). Fig. 10 a) investigates the ρ_{S_φ} based on different SNRs when JSR = 2, 5, 10 dB. It can be increased ρ_{S_φ} in SNR > 9 dB by AWGN noise effects reduction. The highest phase noise power is a little less than the threshold power level, so, the target is detected as a real target. Fig. 10 b) obtains the probability of detection $P_D$based on different SNR. It shows that the accurate detection ($P_D > 90\%$) is achieved when SNR > 9 dB. Similar to the L-band, Fig. 11 a) exhibits the ρ_{S_φ} based on the different time delays (ranges) where the Doppler frequency of the target is 8 KHz, and the SNR is about 15 dB. It can be seen that DRFM phase noise in $R \geq 15$ Km is detectable for discrimination for all ranges. Longer ranges increased the phase noise power. Fig. 11 b) shows the ρ_{S_φ} for various target speeds within 30 km range and SNR is 15 dB. In this result, like in the L-band, the supplementary phase

noise power is more than 4 dB for the DRFM target. Furthermore, higher JSRs made the discrimination better. So, all DRFM targets can be detected under these conditions, and P_D is almost 100%.

Note that, X-band oscillators have additional phase noise power in comparison to L-band oscillators.

VI. CONCLUSION

A novel anti−DRFM jamming method is introduced in this article. The proposed method analyzes the phase noise effects of different oscillators in receiving signals to discriminate targets. Calculating the normalized Euclidean distance difference of the phase noise level of the received signal is proposed for the LFMCW tracking radar sensor networks. The phase noise of DRFM signal and target signal are focused in different situations. It can be seen that a simulated DRFM signal has higher phase noise and changed pattern in comparison to the real target signal. The theoretical analysis investigates the difference between the phase noise level in DRFM−made targets and that of real ones. Then, a simple system is prepared for implementation to measure the phase noise. All phase noise measurements are done through the same sets of circuits and equal time periods. Two operational DRFM systems are produced and used to consider the performance of the proposed method in both the L-band and the X-band. The LRT is used for target discrimination based on a threshold level to achieve the acceptable P_{fa} of target discrimination. All experimental tests proved that the proposed method performs well in different ranges, Doppler frequencies, SNRs, and SJRs. Based on the experimental results, the proposed method can be utilized in discriminating among real and the false targets with high P_D, particularly when the SNR is greater than 10 dB. The simple compatible structure is another advantage of the proposed technique. Finally, this method can be extended using in wireless sensor networks and communication systems to recognize the interference and jamming signals.

ACKNOWLEDGMENT

We gratefully thank of very useful discussions of reviewers. We would like also like to thank from Isfahan University Radar Research Center for providing us the opportunity to work on this extensive research project and allowing us to utilize research facilities to the best of their capabilities.

REFERENCES

[1] J. Scheer and W. L. Melvin, *Principles of Modern Radar*. Edison, NJ, USA: IET Scitech Publishing, 2014.
[2] Y.-X. Zhang, Q.-F. Liu, R.-J. Hong, P.-P. Pan, and Z.-M. Deng, "A novel monopulse angle estimation method for wideband LFM radars," *Sensors*, vol. 16, no. 6, p. 817, p. 2016.
[3] A. T. Elsworth, *Electronic Warfare*. New York, NY, USA: Nova Science Publishers, 2010.
[4] K. T. Zhao, K. Tian, and N. Xu, "New jamming scenario: From marginal jamming to deep jamming," *Phys. Rev. Lett.*, vol. 106, no. 12, p. 125503, 2011.
[5] S. J. Roome, "Digital radio frequency memory," *Electron. Commun. Eng. J.*, vol. 2, no. 4, pp. 147–153, 1990.
[6] V. Sokolovic and V. Popovic, "Radar detection zone under active jamming," *Vojnotehnicki Glasnik*, vol. 57, pp. 58–79, Sep. 2009.
[7] Y. H. Hu, Y. Zheng, and Y. K. Deng, "A study on ECCM using hyperchaotic phase modulated signal," *J. Electron. Inf. Technol.*, vol. 30, pp. 1756–1759, Sep. 2008.
[8] H. Quan, H. Zhao, and P. Cui, "Anti-jamming frequency hopping system using multiple hopping patterns," *Wireless Pers. Commun.*, vol. 81, no. 3, pp. 1159–1176, 2014.
[9] M. S. Popper and S. Capkun, "Anti-jamming broadcast communication using uncoordinated spread spectrum techniques," *IEEE J. Select. Areas Commun.*, vol. 28, no. 5, pp. 703–715, May 2010.
[10] J. Zhang, X. Zhu, and H. Wang, "Adaptive radar phase-coded waveformdesign," *Electron. Lett.*, vol. 45, no. 20, p. 1052, 2009.
[11] J. Akhtar, "Orthogonal block coded ECCM schemes against repeat radar jammers," *IEEE Trans. Aerosp. Electron. Syst.*, vol. 45, no. 3, pp. 1218–1226, Mar. 2009.
[12] Z. Liu, W. Xi-Zhang, and L. Xiang, "Novel method of unambiguous moving target detection in pulse-Doppler radar with random pulse repetition interval," *J. RADARS*, vol. 1, no. 1, pp. 28–35, 2012.
[13] J.-P. Kauppi, K. Martikainen, and U. Ruotsalainen, "Hierarchical classificationof dynamically varying radar pulse repetition interval modulationpatterns," *Neural Netw.*, vol. 23, no. 10, pp. 1226–1237, 2010.
[14] M. Soumekh, "SAR-ECCM using phase-perturbed LFM chirp signals and DRFM repeat jammer penalization," *IEEE Trans. Aerosp. Electron. Syst.*, vol. 42, no. 1, pp. 191–205, Jan. 2006.
[15] J. Su, H.-H. Tao, X.-L. Guo, J. Xie, and X. Rao, "Coherently integrated-cubic phase function for multiple LFM signals analysis," *Electron. Lett.*, vol. 51, no. 5, pp. 411–413, 2015.
[16] H. Esmaeili-Najafabadi, M. Ataei, and M. F. Sabahi, "Designing sequence with minimum PSL using Chebyshev distance and its application for chaotic MIMO radar waveform design," *IEEE Trans. Signal Process.*, vol. 65, no. 3, pp. 690–704, Mar. 2016.
[17] M. Greco, F. Gini, and A. Farina, "Radar detection and classification of jamming signals belonging to a cone class," *IEEE Trans. Signal Process.*, vol. 54, no. 5, pp. 1984–1993, May 2008.
[18] M. Nouri, M. Mivehchy, and S. A. Aghdam, "Adaptive time-frequency Kernel local fisher discriminant analysis to distinguish range deception jamming," in *Proc. IEEE 6th Int. Conf. Comput. Commun. Netw. Technol. (ICCCNT)*, Sep. 2015, pp. 1–5.
[19] K. Kundert. (2003). *Predicting the Phase Noise and Jitter of PLL-Based Frequency Synthesizers*. [Online]. Available: http://www.designers-guide.com
[20] A. Chorti and M. Brookes, "A spectral model for RF oscillators with power-law phase noise," *IEEE Trans. Circuits Syst.*, vol. 53, no. 9, pp. 1989–1999, Sep. 2006.
[21] G. Klimovitch, "A nonlinear theory of near-carrier phase noise in freerunning oscillators," in *Proc. IEEE Int. Conf. Circuits Syst.*, Mar. 2000, pp. 1–6.
[22] L. Tomba, "On the effect of Wiener phase noise in OFDM systems," *IEEE Trans. Commun.*, vol. 46, no. 5, pp. 580–583, May 1998.
[23] G. Niu, "Noise in SiGe HBT RF technology: Physics, modeling, and circuit implications," *Proc. IEEE*, vol. 93, no. 9, pp. 1583–1597, Sep. 2005.
[24] A. Demir, A. Mehrotra, and J. Roychowdhury, "Phase noise in oscillators: A unifying theory and numerical methods for characterization," *IEEE Trans. Circuits Syst.*, vol. 47, no. 5, pp. 655–674, May 2000.
[25] L. Wu, S. S. Peng, and X. Q. Shi, "Effects of transmitter phase noise on millimeter wave LFMCW radar performance," in *Proc. IEEE Int. Microw. Millim. Wave Technol. Conf. Dig.*, Oct. 2008, pp. 1415–1418.
[26] K. Olivier and M. Gouws, "Modern wideband DRFM architecture and real-time DSP capabilities for radar test and evaluation," in *Proc. Saudi Int. Electron. Commun. Photon. Conf.*, Apr. 2013, pp. 1–4.
[27] M. I. Skolnik, "Introduction to radar," in *Radar Handbook*, vol. 2. New York, NY, USA: McGraw-Hill, 1962.
[28] H. Gheidi and A. Banai, "Phase-noise measurement of microwave oscillators using phase-shifterless delay-line discriminator," *IEEE Trans. Microw. Theory Techn.*, vol. 58, no. 2, pp. 468–477, Feb. 2010.
[29] E. Rubiola and V. Giordano, "Advanced interferometric phase and amplitude noise measurements," *Rev. Sci. Instrum.*, vol. 73, no. 6, pp. 2445–2457, 2002.
[30] F. L. Walls, "Secondary standard for PM and AM noise at 5, 10, and 100 MHz," *IEEE Trans. Instrum. Meas.*, vol. 42, no. 2, pp. 136–143, Apr. 1993.
[31] E. Rubiola, *Phase Noise and Frequency Stability in Oscillators*. Cambridge, U.K.: Cambridge Univ. Press, 2008.
[32] *Practical Considerations for Modern RF & Microwave Phase Noise Measurement Seminar*, Hewlett-Packard Company, Palo Alto, CA, USA, 1998.

[33] R. Boudot and E. Rubiola, "Phase noise in RF and microwave amplifiers," *IEEE Trans. Ultrason., Ferroelect., Freq. Control*, vol. 59, no. 12, pp. 2613–2624, Dec. 2012.
[34] A. S. Gupta, D. A. Howe, C. Nelson, A. Hati, F. L. Walls, and J. F. Nava, "High spectral purity microwave oscillator: Design using conventional air-dielectric cavity," *IEEE Trans. Ultrason., Ferroelect., Freq. Control*, vol. 51, no. 10, pp. 1225–1231, Oct. 2004.
[35] A. Brannon, J. Breitbarth, and Z. Popovic, "A low-power, low phase noise local oscillator for chip-scale atomic clocks," in *IEEE MTT-S Int. Microw. Symp. Dig.*, Jun. 2005, pp. 1535–1538.
[36] C. Azeredo-Leme, "ADC performance: What's jitter got to do with it?" *Electronic Design*, 2017. [Online]. Available: http://www.electronicdesign.com/analog/adc-performance-what-s-jitter-got-do-it
[37] M. Nouri, M. Mivehchy, and M. F. Sabahi, "Jammer target discrimination based on local variance of signal histogram in tracking radar and its implementation," *Signal, Image Video Process.*, pp. 1–8, Feb. 2017, doi: 10.1007/s11760-016-1053-8.

MAHDI NOURI (S'10) was born in Iran, in 1987. He received the B.S. degree in communication engineering from the University of Tabriz, Tabriz, Iran, in 2009, and the M.S. degree in secure communication engineering from the Iran University of Science & Technology, Tehran, Iran, in 2012. He is currently pursuing the Ph.D. degree with Electrical Engineering Department, University of Isfahan. He was a Research Assistant with the Tehran Academy of Sciences and Iran Telecommunication Research Center, Iran, in 2011–2012. He is a Teaching Assistant with Electrical Engineering Department, University of Isfahan, since 2013. He is currently a member of the Iran National Foundation of Elites. His research interests are in the areas of radar signal processing, signal processing for wireless and optical communication systems, audio and speech processing, STBC channel coding, and channel modeling.

MOHSEN MIVEHCHY (M'15) received the B.E. degree in electronic engineering and the M.E. degree in communication engineering from the Isfahan University of Technology, Isfahan, Iran, in 1987 and 1990, respectively, and the Ph.D. degree in electrical engineering from the University of Isfahan (UI), Iran, in 2010. He is currently an Assistant Professor with Electrical Engineering Department, UI, and the Head of RF and Communication Circuits Research Center, since 2004. His long time practical experiences and research interest include high frequency circuits design and radar system.

MOHAMAD F. SABAHI was born in Isfahan in 1976. He received the B.S. degree in electronics engineering, the M.S. degree in communication engineering, and the Ph.D. degree in electrical engineering from the Isfahan University of Technology, Isfahan, Iran, in 1998, 2000, and 2008, respectively. He has been a Faculty Member with Electrical Engineering Department, University of Isfahan, since 2008. His main research interests include statistical signal processing, detection theory, and wireless communication.